ACI MATERIALS JOURNAL TECHNICAL PAPER

Title no. 85-M32

# Effect of Temperature and Humidity on Fracture Energy of Concrete

by Zdeněk P. Bažant and Pere C. Prat

*Fracture experiments were conducted at temperatures from 20 to 200 C (68 to 392 F) to determine the dependence of the Mode I fracture energy of concrete on temperature as well as the specific water content. The fracture energy values were determined by testing geometrically similar specimens of sizes in the ratio 1:2:4:8 and then applying Bažant's size effect law. Three-point bend specimens and eccentric compression specimens are found to yield approximately the same fracture energies, regardless of temperature. To describe the temperature dependence of fracture energy, a recently derived simple formula based on the activation energy theory (rate process theory) is used and verified by test results. The temperature effect is determined both for concrete predried in an oven and for wet (saturated) concrete. By interpolation, an approximate formula for the effect of moisture content on fracture energy is also obtained. This effect is found to be small at room temperature but large at temperatures close to 100 C (212 F).*

**Keywords: concretes; cracking (fracturing); energy**; humidity; moisture content; temperature.

While heating in metals causes abrupt increases of fracture toughness, due to brittle-ductile transitions which change the fracture mechanism, the fracture toughness of purely brittle materials such as glass, ceramics, graphite, and rocks is known to smoothly decrease with increasing temperature[1-3]. For concrete, the determination of the influence of temperature on the fracture energy has been hampered by the fact that until recently an unambiguous definition and method of measurement of the fracture energy itself was unavailable. The basic classical measurement methods, such as the work of fracture method proposed for concrete by Hillerborg et al.[4,5] and adopted by The International Union of Testing and Research Laboratories for Materials and Structures (RILEM) or the methods based on compliance or crack opening displacement measurements, have not been found to yield the same fracture energy values when specimens of significantly different sizes or shapes were used.

Recently, however, a fracture energy definition that leads to unique values has been proposed.[6-10] The fracture energy is the specific energy required for fracture growth in an infinitely large specimen. This definition obviously requires knowledge of the size effect law which has to be used to extrapolate the test results to infinite size. Although the exact size effect law is unknown, the approximate Bažant's law[11] has been found to be sufficient in view of the inevitable statistical scatter of concrete.[6,7,10,12-14]

Measurements of concrete fracture energy based on extrapolation to infinite size were made by Bažant, Kim, and Pfeiffer.[9,10] Bažant and Pfeiffer[15] experimentally demonstrated that specimens of very different types, including the three-point bend specimens, edge-notched tensile specimens, and eccentric compression specimens, yield approximately the same fracture energy values, as far as the typical scatter exhibited by concrete permits one to discern. As for the effect of specimens size on fracture energy, none can be present due to the very nature of this fracture energy definition.

The availability of a measurement method that yields unique values of fracture energy makes it meaningful to study various factors that influence fracture energy. The objective of this study is to examine the effect of temperature as well as the related effect of humidity. The values of fracture energy need to be known to predict brittle failures of concrete structures on the basis of fracture mechanics, which promises to give more accurate results than the methods of limit analysis.

## EXPERIMENTAL INVESTIGATION

The test specimens were beams of constant rectangular cross section loaded at three points [Fig. 1(a)]. To determine the size effect, geometrically similar specimens of various depth $d$ were used. The depths were $d$

Received Feb. 4, 1987, and reviewed under Institute publication policies.
 Pertinent discussion will be published in the May-June 1989 *ACI Materials Journal* if received by Feb. 1, 1989.

*Zdeněk P. Bažant, FACI, has been a professor at Northwestern University since 1973 and has also served there as director of the Center for Concrete and Geomaterials. He currently is Professor and Director, the Technological Institute, Department of Civil Engineering, Northwestern University. He is a registered structural engineer and a consultant to Argonne National Laboratory and several other firms and is on editorial boards of six journals. He is Chairman of ACI Commmittee 446, Fracture Mechanics; and is a member of ACI Committees 209, Creep and Shrinkage in Concrete; and 348, Structural Safety. Currently he is Chairman of RILEM Committee TC69 on creep and of IA-SMiRT Division H. In 1987, Professor Bažant visited the University of Tokyo as Kajima Foundation Fellow and during 1988 he is a NATO Senior Guest Scientist at E.N.S., Paris-Cachan.*

*ACI member Pere C. Prat is a research associate at the Materials Science Institute (CSIC), Barcelona, Spain. He obtained his civil engineering degree from the School of Civil Engineering of the Technical University of Catalonia, Barcelona, Spain, and his PhD from Northwestern University. His research interests include constitutive models for geomaterials, strain-softening behavior, fracture mechanics, nonlinear analysis of concrete structures, experimental methods, and finite element applications.*

= 1.5, 3, 6, and 12 in. (38.1, 76.2, 152, and 305 mm), while the thickness was $b$ = 1.5 in. (38.1 mm) for all the specimens. The length-to-depth ratio was $L/d$ = 8:3 and the span-to-depth ratio was $\ell/d$ = 2.5, for all specimens. One notch of depth $d/6$ and thickness 0.1 in. (2.5 mm) (same for all specimens) was cut with a diamond saw three weeks after the specimens were stripped from the molds.

To check for a possible effect of specimen type, additional specimens of the same shape were tested in eccentric compression. These specimens, which had two symmetrical notches of depth $d/6$ and thickness 0.1 in. (2.5 mm) [Fig. 1(b)], included only specimen sizes $d$ = 1.5, 3, and 6 in. ($d$ = 12 in. would not fit the available oven).

From each batch of concrete, one specimen of each size as well as three control cylinders for compression strength, 3 in. (152 mm) in diameter and 6 in. (305 mm) in length, were cast. The means and standard deviations of the compression strengths after 28 days of moist curing are given in Table 1.

All specimens were cast with the side of depth $d$ in the vertical position, using a water-cement ratio of 0.6 and a cement-sand-gravel ratio of 1:2:2 (all by weight). The maximum gravel size was $d_a$ = 0.5 in. (12.7 mm) and the maximum sand grain size was 0.19 in. (4.8 mm). The aggregate consisted of crushed limestone and siliceous Illinois beach sand (Lake Michigan). Portland cement C 150 (ASTM Type I), with no admixtures and no air-entraining agents, was used.

The fracture specimens were removed from the plywood forms after one day and subsequently cured until about 2 hr before the test in a moist room with 95 percent humidity and a temperature of 25 C (77 F). Three identical specimens were cast simultaneously from each successive batch for each type of test. The age of the specimens at the time of the test was 28 days, except for the specimens tested in the hot water bath. For these, the tests had to be postponed to the age of 41 days due to certain scheduling problems.

The fracture tests were carried out at two types of humidity conditions — dry and wet. The dry tests included both the three-point loaded specimens and eccentric compression specimens. The temperatures in these tests were 20 C (68 F), 65 C (149 F), 120 C (248 F), and 200 C (392 F). Each of the tests started with preheating under no load in an oven. The temperature in the oven was raised gradually over a period of about 1 hr to the temperature of 120 C, which was then kept for 3 hr. The specimens were not sealed and may be expected to have lost all their evaporable water. After this

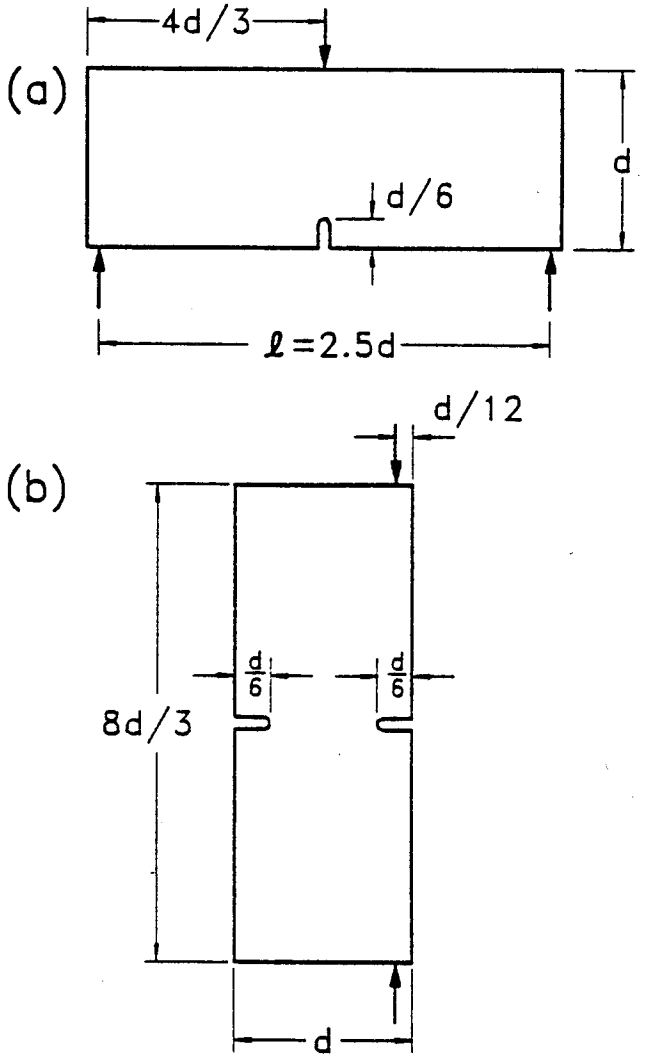


*Fig. 1—Test specimens used: (a) three-point bend specimens; and (b) eccentric compression specimens*

**Table 1 — Compression strength of concrete (on 3 × 6-in. cylinders) in psi***

| Test series | Mean $f'_c$ | Standard deviation $s$ |
|---|---|---|
| 3-point bend, dry, 20 C | 5550 | 36 |
| 3-point bend, dry, 65 C | 5585 | 139 |
| 3-point bend, dry, 120 C | 4975 | 90 |
| 3-point bend, dry, 200 C | 5000 | 95 |
| Eccentric compression, dry, 20 C | 5410 | 78 |
| Eccentric compression, dry, 65 C | 5250 | 59 |
| Eccentric compression, dry, 120 C | 5075 | 117 |
| Eccentric compression, dry, 200 C | 5075 | 90 |
| 3-point bend, wet, 65 C† | 5770 | 55 |
| 3-point bend, wet, 90 C‡ | 5725 | 84 |

* 1 psi = 6895 Pa.
† Corrected for age; measured was $f'_c$ = 6035 psi, $s$ = 58 psi at 41 days.
‡ Corrected for age; measured was $f'_c$ = 5990 psi, $s$ = 88 psi at 41 days.

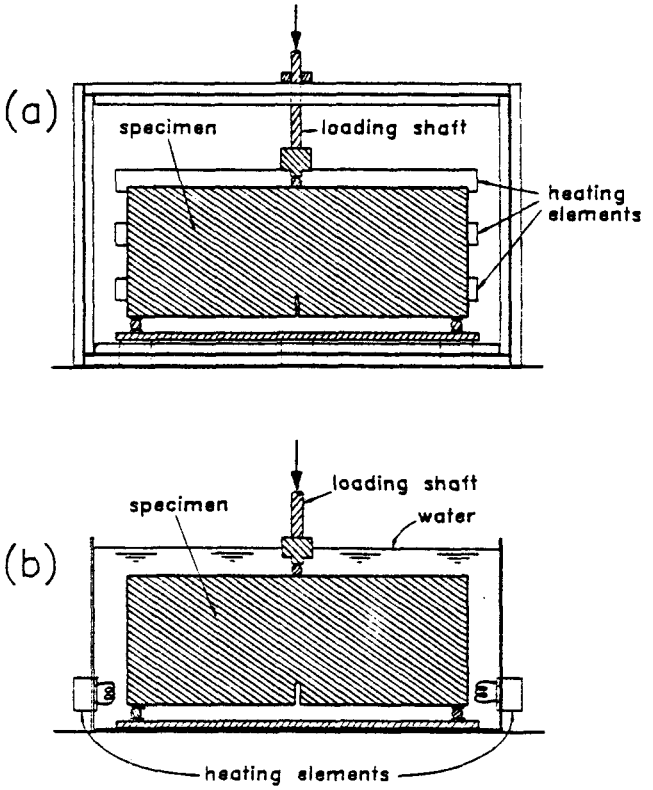


*Fig. 2—Arrangement of tests: (a) in an oven; and (b) in a water bath*

3 hr period, the temperature was gradually raised or lowered at the average rate of about 50 C/hr (90 F/hr), until the desired temperature of the fracture test was reached. The specimen was then loaded to failure while in the oven [Fig. 2(a)]. The loading shaft of the machine protruded through the wall of the oven, and the thermal insulation around the shaft caused no appreciable friction.

According to the linear heat conduction equation and the known thermal diffusivity of concrete, it was calculated that, after a sudden exposure to a different constant temperature, not more than 1 hr is needed for the temperature to become uniform within the specimen of thickness 1.5 in. (38.1 mm). Therefore, the heating times used must have been sufficient. The heating time in the oven must have also sufficed, since a uniformly dry state throughout the specimen thickness was obtained. This is not only well known empirically but is also justified by the measurements and theory in Reference 16, in which it was found that the diffusivity of moisture in concrete increases about 200 times when the temperature exceeds 100 C (212 F).

Although concrete drying by heating in an oven has been a standard practice in the investigations of creep and other properties, this procedure might, nevertheless, cause some damage such as microcracking and, thus, possibly affect the fracture test results. However, the fact that after such drying, the fracture energy of concrete becomes much higher than for a wet specimen at the same elevated temperature suggests that possible damage due to heating is probably not serious. The alternative to drying the specimens without heating is hardly feasible. Simplified calculations showed that the previously mentioned heating rates were slow enough to avoid development of high thermal stresses.

The wet tests included only three-point bend specimens. Each test started by placing the specimens into a water-filled tank [Fig. 2(b)] with the water at room temperature. The temperature of the water in the tank was raised gradually, at the rate of about 50 C/hr (90 F/hr), to the desired test temperature and was then kept constant for 1 hr before the fracture test in water was started.

The temperatures of the wet tests were 65 C (149 F) and 90 C (194 F). No wet tests were conducted at room temperature, since the response of wet specimens at room temperature may be assumed to be the same as that of previously tested unsealed and undried specimens, loaded right after curing. This assumption is justified by the fact that at room temperature the moisture diffusion is so slow that the environmental humidity cannot affect the state of concrete in the bulk of the specimen during the short time of exposure. At 120 C (248 F), by contrast, the diffusivity of moisture in concrete is about 200 times higher than it is at 90 C (194 F), and about 3000 times higher than at 20 C (68 F).[16] Therefore, the environmental relative humidity quickly spreads through the entire specimen.

No wet tests could be carried out at temperatures over 100 C (212 F), since the specimen could not be kept wet unless a pressure chamber was used. However, this would represent a different type of test.

All the tests were carried out in a closed-loop MTS machine. Only the maximum load values were needed to calculate the fracture energies. The loading rate was such that the time to failure was 3 to 5 min for all specimens.

All the dry tests were performed under stroke-control at a constant displacement rate. For certain extraneous reasons, the wet specimens had to be tested under load control; therefore, they failed right at the maximum load. Impossible though load-controlled testing is for other types of fracture tests (e. g., RILEM's work of fracture test), it is nevertheless acceptable for the present method since the post-peak response is not needed to determine the fracture energy. Theoretically, if the specimens exhibit high statistical heterogeneity, load-controlled tests can yield a lower maximum load than the displacement-controlled tests, but, according to the analysis of Bažant and Panula,[17] the differences that may reasonably be expected in the maximum load value are insignificant (under 3 percent). On the other hand, if the objective were the post-peak descending load-deflection curve, then load-controlled tests would of course be impossible.

The measured maximum load values $P$ are given in Table 2 and the 28-day compression strengths $f'_c$ for individual batches of concrete in Table 1. The 28-day $f'_c$ values for the wet tests were not directly measured but were calculated from the compression strength $f'_c$ (41) measured at the time of these tests, at which the age of concrete was 41 days. The adjustment for age was

based on the approximate formula[18]

$$f_c'(t) = f_c'(28)[1 + 0.277\log(t/28)]$$
$$\text{from which } f_c'(28) \approx 0.956 f_c'(41)$$

## CALCULATION OF FRACTURE ENERGY FROM SIZE EFFECT

The size effect is the most important difference of fracture mechanics from the failure theories based on plastic limit analysis. The size effect is understood as the dependence of the nominal stress at failure $\sigma_N$ on a characteristic dimension of the specimen $d$ when geometrically similar specimens or structures are considered ($\sigma_N = P/bd$, where $P$ = maximum load and $b$ = specimen thickness). For stress-based failure theories such as the plastic limit analysis or elastic allowable strength design, there is no size effect, i.e., $\sigma_N$ is constant. For classical linear elastic fracture mechanics, $\sigma_N \sim d^{-1/2}$. Due to the influence of a relatively large microcracking zone that blunts the crack front in concrete, the size effect is intermediate between plasticity and linear fracture mechanics and represents a transition from the former to the latter as the size is increased. This transition may be approximately described by Bažant's size effect law:[11] $\sigma_N = Bf_t'(1 + d/\lambda_0 d_a)^{-1/2}$ in which $B$, $\lambda_0$ = empirical constants and $d_a$ = maximum aggregate size. According to this law, the plot of $Y = (f_t'/\sigma_N)^2$ versus $X = d/d_a$ (relative size) should be a straight line $Y = AX + C$, with $C = 1/B^2$ and the slope $A = C/\lambda_0$. Thus, a linear regression of the test results in the plot of $Y$ versus $X$ may be used to determine $A$ and $C$, from which the size effect law parameters may then be calculated as $B = C^{-1/2}$ and $\lambda_0 = C/A$.

These regression plots also yield statistics of the errors, i.e., the deviations of the measured data points from the size effect law. The coefficient of variation, defined as $\omega_{Y|X} = \{[\Sigma(Y_i^{test} - Y_i)^2]/(N-2)\}^{1/2}/\overline{Y}$ where $Y_i^{test} - Y_i$ are the vertical deviations of data points $Y_i^{test}$ from the regression line, $N$ is the number of all the data points, and $\overline{Y} = (\Sigma Y_i)/N$ = mean of all measured $Y_i$, is given in Fig. 3, 4, and 5, as is the correlation coefficient $r$.

From the size effect law, it follows[8-10] that the fracture energy $G_f$, defined as the energy release rate required for crack growth in an infinitely large specimen, may be calculated from the formula

$$G_f = \frac{g(\alpha_0)}{AE_c} f_t'^2 d_a \qquad (1)$$

in which $\alpha_0 = a_0/d$; $a_0$ = notch length; $d$ = beam depth; $E_c$ = modulus of elasticity of concrete; $f_t'$ = direct tensile strength of concrete; $A = 1/(B^2\lambda_0)$ = slope of the regression line as already defined; $g(\alpha_0)$ = nondimensional energy release rate of the specimen according to the linear elastic fracture mechanics, which can be found for the basic specimen geometries in textbooks[19,20] and handbooks,[21] and can be, in general, determined by linear finite element analysis. For the three-point specimens used, $g(\alpha_0) = 6.37$, and for the eccentric compression specimens, $g(\alpha_0) = 1.68$.

**Table 2 — Maximum loads at failure**

| Type of test | Depth, in. | Load at failure $P$, lb 1 | 2 | 3 | Average $P$, lb |
|---|---|---|---|---|---|
| Three-point bend Dry, 20 C | 1.5 | 390 | 420 | 375 | 395 |
| | 3.0 | 645 | 690 | 675 | 670 |
| | 6.0 | 990 | 1035 | 1080 | 1035 |
| | 12.0 | 1710 | 1689 | 1729 | 1709 |
| Three-point bend Dry, 65 C | 1.5 | 515 | 375 | 440 | 443 |
| | 3.0 | 715 | 565 | 670 | 650 |
| | 6.0 | 1090 | 955 | 1155 | 1066 |
| | 12.0 | 1595 | 1430 | 1600 | 1542 |
| Three-point bend Dry, 120 C | 1.5 | 348 | 384 | 366 | 366 |
| | 3.0 | 530 | 594 | 486 | 537 |
| | 6.0 | 954 | 840 | 864 | 886 |
| | 12.0 | 1296 | 1368 | 1332 | 1332 |
| Three-point bend Dry, 200 C | 1.5 | 304 | 322 | 320 | 315 |
| | 3.0 | 540 | 480 | 510 | 510 |
| | 6.0 | 792 | 744 | 816 | 784 |
| | 12.0 | 1180 | 1190 | 1200 | 1190 |
| Eccentric compression Dry, 20 C | 1.5 | 675 | 665 | 690 | 677 |
| | 3.0 | 1180 | 1160 | 1260 | 1200 |
| | 6.0 | 2040 | 2195 | 1945 | 2060 |
| Eccentric compression Dry, 65 C | 1.5 | 855 | 715 | 594 | 721 |
| | 3.0 | 1280 | 1223 | 1080 | 1194 |
| | 6.0 | 2100 | 2010 | 1740 | 1950 |
| Eccentric compression Dry, 120 C | 1.5 | 740 | 775 | 680 | 732 |
| | 3.0 | 1140 | 1240 | 1215 | 1198 |
| | 6.0 | 1860 | 1920 | 1720 | 1833 |
| Eccentric compression Dry, 200 C | 1.5 | 648 | 684 | 720 | 684 |
| | 3.0 | 960 | 960 | 900 | 940 |
| | 6.0 | 1545 | 1705 | 1625 | 1625 |
| Three-point bend Wet, 65 C | 1.5 | 342 | 390 | 408 | 380 |
| | 3.0 | 545 | 546 | 586 | 559 |
| | 6.0 | 811 | 780 | 732 | 774 |
| | 12.0 | 1250 | 1205 | 1210 | 1222 |
| Three-point bend Wet, 90 C | 1.5 | 290 | 350 | 290 | 310 |
| | 3.0 | 560 | 520 | 575 | 552 |
| | 6.0 | 640 | 690 | 745 | 692 |
| | 12.0 | 1055 | 1060 | 1010 | 1042 |

1 in. = 25.4 mm. 1 lb. = 4.448 N.

The tensile strength was not measured but was estimated from the formula $f_t' \approx 6(f_c')^{1/2}$ where $f_c'$ and $f_t'$ are in psi, $f_c'$ = compression strength. A possible error in the $f_t'$-value, however, has no effect on $G_f$ since the $A$-value obtained by regression is proportional to $f_t'^2$ if the ordinate is taken as $Y = f_t'^2/\sigma_N^2$.

Fig. 6 is a photograph of a typical set of specimens of different sizes. Fig. 7 shows typical specimens installed in the heating oven, and Fig. 8 shows typical specimens installed in the water bath.

The maximum loads measured are plotted in Fig. 3 through 5. The plots on the right demonstrate that the measured $\sigma_N$ agrees quite well with the size effect law, which is shown as the solid curve. This agreement justifies the use of the size effect law. The plots on the left show the linear regressions that yield the optimum values of parameters $B$ and $\lambda_0$. The fracture energy values calculated according to Eq. (1) from the Slopes $A$ of the regression lines given on the left of Fig. 3 through 5 are tabulated in Table 3.

Since the wet specimens had to be tested at the age of 41 days rather than 28 days, a correction for the age difference became necessary. The fracture energy values were transformed to 28 days according to Bažant

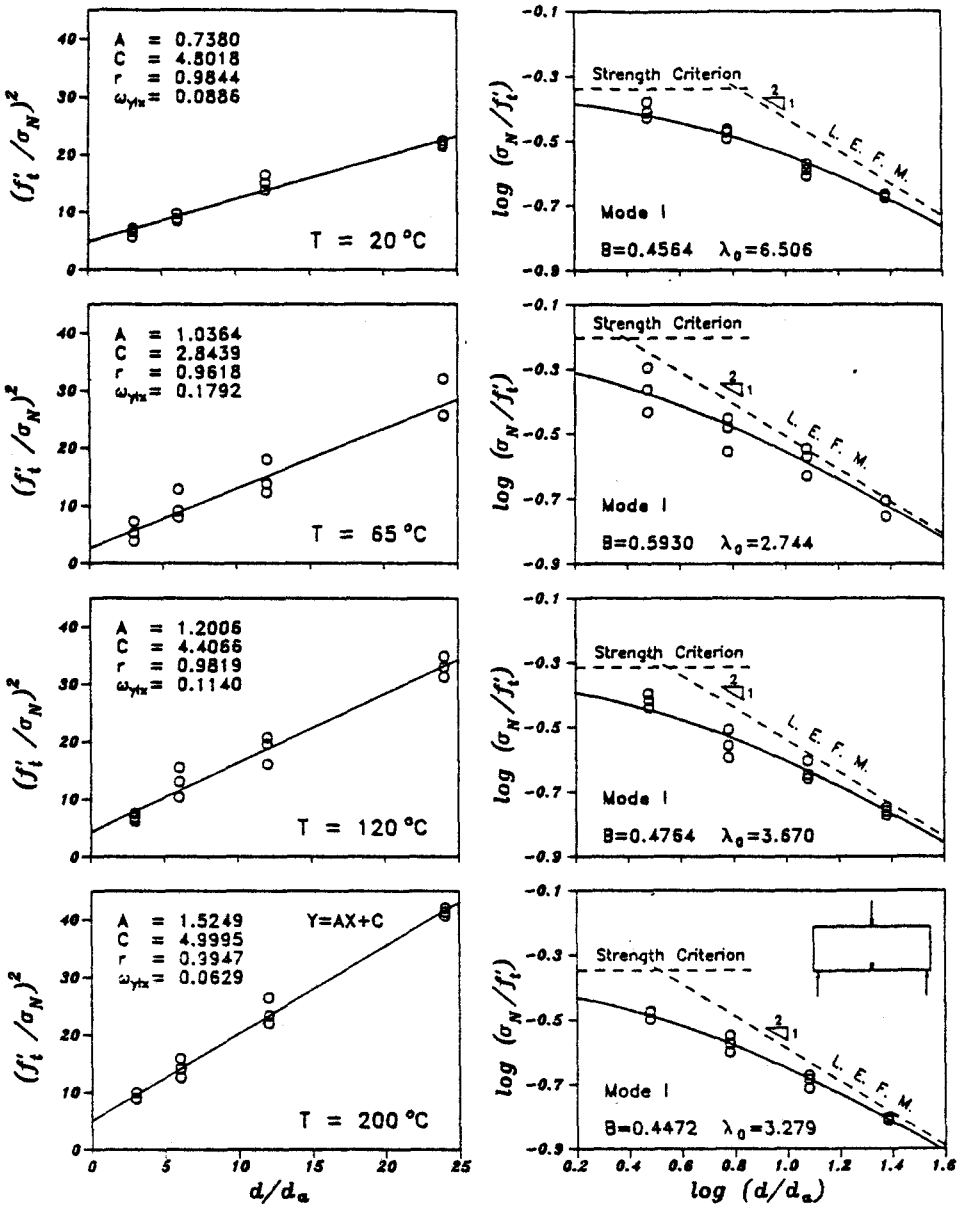


*Fig. 3—One set of three-point bend specimens tested*

and Oh's approximate formula[22] $G_f = (2.72 + 0.0214 f_t') f_t'^2 d_a/E$. The values in Tables 1 and 3 as well as those plotted in the figures are all transformed to 28 days.

## ACTIVATION ENERGY FORMULATION

It is generally accepted that fracture is a thermally activated rate process. This means that the atomic bond ruptures that constitute the mechanism of fracture are provoked by the energies of thermal vibrations.[23] These energies are statistically distributed, as described by Maxwell distribution, and a rise in temperature increases the probability (or frequency) that the atom's energy would exceed the activation energy barrier of the bond. Therefore, a rise in temperature causes an increase in the rate of growth of fracture, which generally follows a formula of the type $\dot{a} = f(K) \exp(-U/RT)$,[3] where $U$ = activation energy of bond rupture; $R$ = universal gas constant; $T$ = absolute temperature; $K$ = stress intensity factor; and $f(K)$ = empirical monotonically increasing function. Recently, Evans[24] and Thouless et al.[25] verified for certain ceramics a special form of this formula

$$\dot{a} = v_c (K/K_c)^n e^{-U/RT} \quad (2)$$

in which $v_c$ and $n$ may be approximately considered as constants characterizing the given material and $K_c$ = critical value of $K$ (fracture toughness). Since concrete is a ceramic material, Eq. (2) may be expected to apply also. This equation is not exact but approximate only, for two reasons: 1) the proportionality of $\dot{a}$ to $K^n$ is empirical; and 2) more than one mechanism of atomic bond rupture, with different activation energies, might be involved, and the type of this mechanism might change with temperature.

Due to the relations $K = (GE_c)^{1/2}$ and $K_c = (G_f E_c)^{1/2}$, where $G$ = rate of energy release from the structure

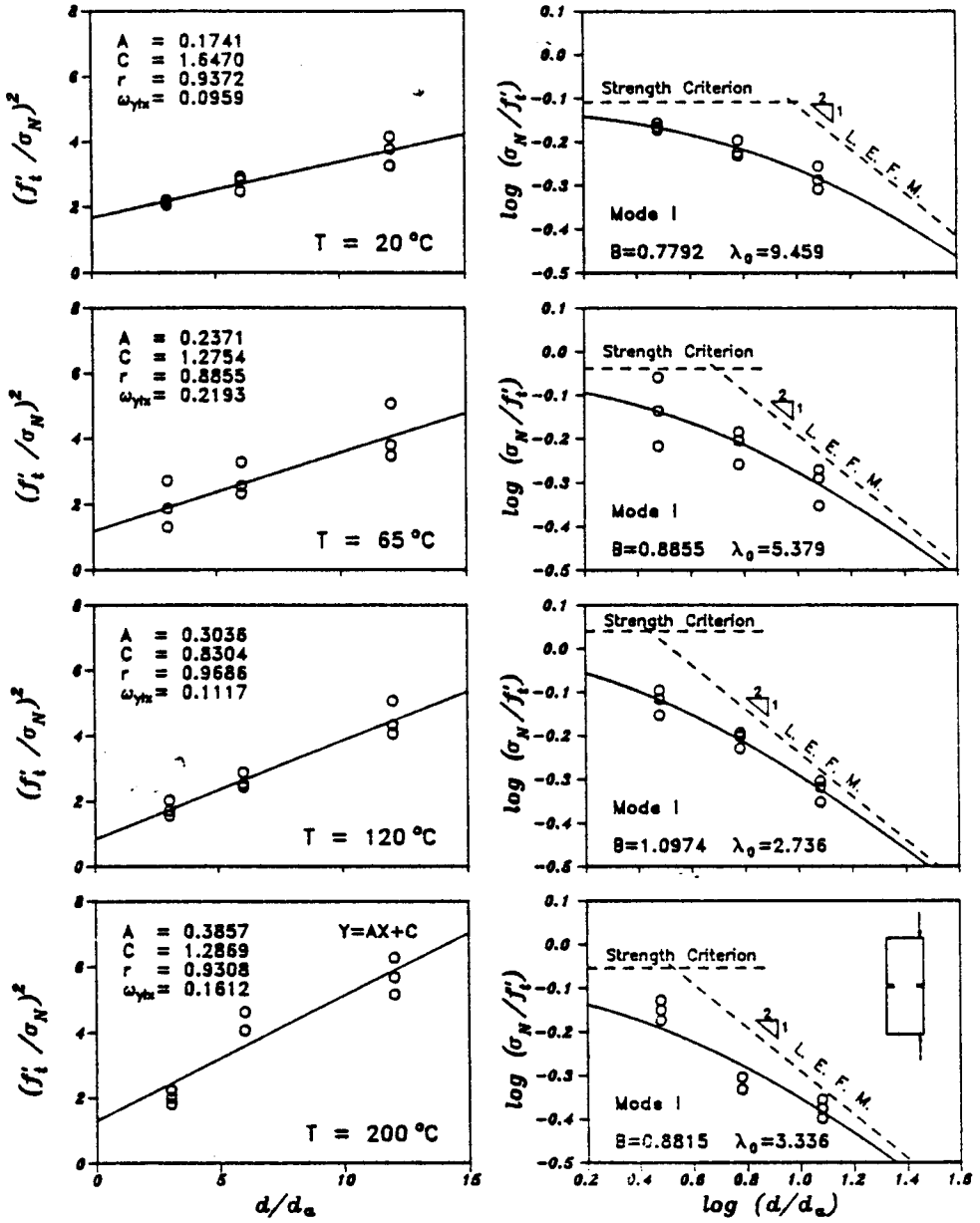


*Fig. 4—Test results for dry eccentric compression specimens*

into the fracture process zone,[19,20] Eq. (2) may be rewritten as

$$\dot{a} = v_c \left(\frac{G}{G_f^\circ}\right)^{n/2} \exp\left[-\frac{U}{R}\left(\frac{1}{T} - \frac{1}{T_0}\right)\right] \qquad (3)$$

where $T_0$ = chosen reference temperature (normally $T_0 = 298$ K) and $G_f^\circ$ = value of fracture energy $G_f$ at $T_0$. With regard to the finite size of fracture process zone in concrete, the relation $K = (GE_c)^{1/2}$ might at first be deemed inconsistent since it is based on linear elastic fracture mechanics. It is nevertheless consistent since, according to the size effect law, $G$ is defined as the fracture energy of an infinitely large specimen, for which linear elastic fracture mechanics does apply.

Eq. (2) or (3) may serve as the basic relation for crack growth in time. Although the time-dependent fracture description in terms of the crack growth rate is no doubt physically more fundamental, the time-independent fracture description prevails in applications. In fact, what is known as fracture mechanics is a time-independent theory. So, deduction of the consequences of Eq. (2) for time-independent fracture description is needed. This was done in Reference 8.

The choice of the reference temperature $T_0$ in Eq. (3) is arbitrary. If temperature $T$ is chosen as the reference temperature, then according to Eq. (3) the crack growth rate $\dot{a}$ at temperature $T$ is simply expressed as

$$\dot{a} = v_c (G/G_f)^{n/2} \qquad (4)$$

(because $1/T_0 - 1/T = 0$ in this case). $G_f$ represents the fracture energy at temperature $T$, while $G_f^\circ$ is the fracture energy at temperature $T_0$.

The crack growth rate expressions referred to $T_0$ or to $T$ must be equivalent. Equating the expressions in Eq. (3) and (4), one obtains Bažant's[3] approximate formula

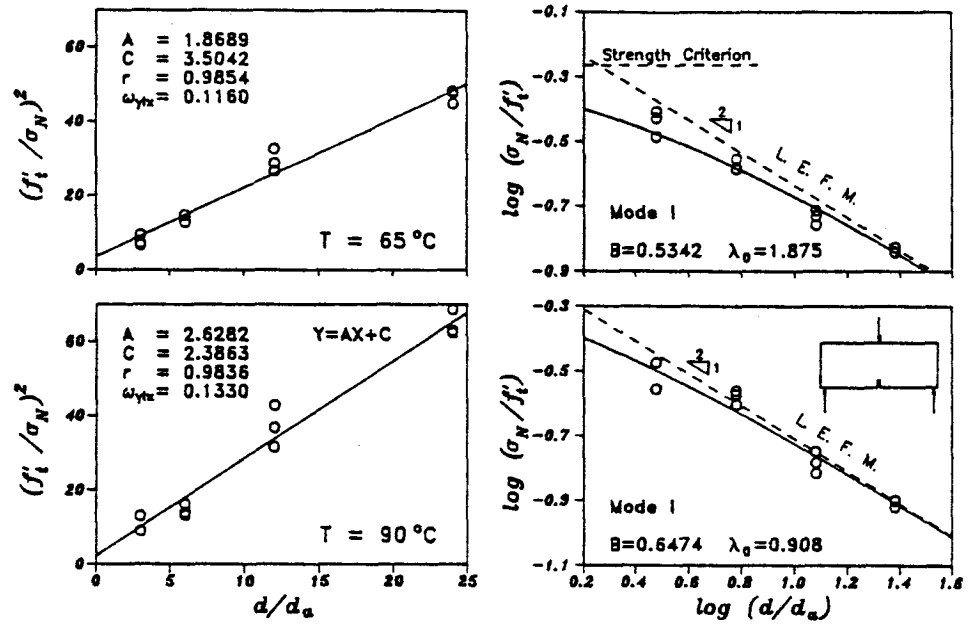


*Fig. 5—Test results for wet three-point bend specimens*

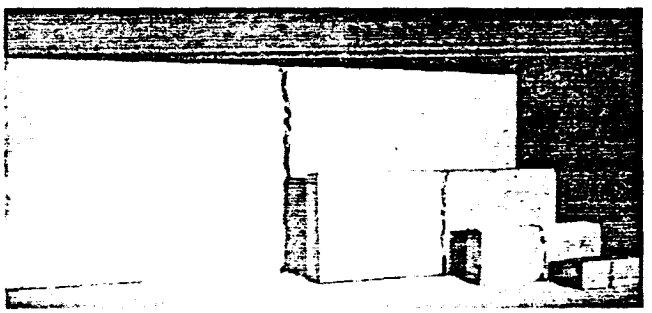

*Fig. 6—One set of three-point bend specimens tested*

$$G_f = G_f^\circ \exp(\gamma/T - \gamma/T_0) \quad (5)$$

in which

$$\gamma = 2U/nR \quad (6)$$

$\gamma$ is a constant characterizing the given material.

Eq. (5) allows a simple determination of material parameters since it may be written in the form $Y = \gamma X + b$ where $Y = ln\ G_f^\circ$; $X = 1/T$; $b = ln\ G_f^\circ - \gamma/T_0$. So the values of $\gamma$ and $b$ may be found as the slope and the Y-intercept of the regression line in the plot of $ln\ G_f$ versus $1/T$, and $G_f^\circ = \exp(b + \gamma/T_0)$.

The values of activation energy $U$ cannot be determined from the present types of experiments. According to Eq. (6), one would also need to determine exponent $n$. This would require measuring the rate of growth of the crack length at various load values.

The fracture energy values obtained experimentally at various temperatures are plotted in Fig. 9(b) as the data points. The linear regression plot, shown in Fig. 9(a), demonstrates that the present test results indeed fall quite close to a straight line in this plot. This confirms the validity of Eq. (5). The diagram on Fig. 9(b) shows the curves of Eq. (5) plotted for the optimum material parameter values of $\gamma$ and $G_f^\circ$ obtained by linear regression. These values are (1 N/m = 0.005710 lb/in.):

Three-point bend, dry: $G_f^\circ = 34.48$ N/m, $\gamma = 581$ K
Eccentric compression,
dry: $G_f^\circ = 38.39$ N/m, $\gamma = 623$ K
Average of dry tests: $G_f^\circ = 36.38$ N/m, $\gamma = 602$ K
Three-point bend, wet: $G_f^\circ = 33.03$ N/m, $\gamma = 1875$ K

Note that the differences between the two specimen shapes (dry tests) are statistically insignificant, in view of the usual scatter for concrete. They are ± 5.5 percent for $G_f^\circ$ and ± 3.5 percent for $\gamma$, relative to the means. Since there is no significant difference between the eccentric compression and three-point bend dry tests, a combined line for both is plotted in Fig. 9(b), according to Eq. (5). The fracture energy $G_{f,dry}$ at reference temperature $T_0$ = 20 C (68 F) is obtained by linear regression using the combined data of both tests.

The portion of the wet specimen curve that lies above the temperature of 100 C (212 F) in Fig. 9(a) is strictly hypothetical because concrete cannot hold evaporable water above 100 C (unless the test was made in a pressurized chamber, but that would change $G_f$ as well). Therefore, wet fracture energy for static loading above 100 C is physically meaningless.

For wet concrete at temperatures below about 20 C, Eq. (5) is probably inapplicable since the wet specimen curve in Fig. 9(a) would pass above the dry specimen curve. This would contradict the fact that the presence of moisture is known to weaken the bonds in hydrophilic porous solids.

Based on the previous results, the effect of the evaporable water content of concrete $w$ per unit volume of concrete may be estimated. Let $\gamma_0$ and $\gamma_1$ be the values of $\gamma$ at $w = 0$ (dry state) and at $w = w_1$ = saturation water content (wet state). As a crude estimate, we may assume a linear variation of $\gamma$ as function of $w$. This

yields for any water content the approximation

$$\gamma = \gamma_0 + (\gamma_1 - \gamma_0)\frac{w}{w_1} \quad (7)$$

According to the results shown $\gamma_0 = 602$ K and $\gamma_1 = 1875$ K for the concrete tested.

The dependence of $\gamma$ on $w$ may be physically explained by a dependence of the activation energy $U$ on $w$. Such a dependence is reasonable to expect since it is known that the activation energy of concrete creep depends on $w$. According to Eq. (7), we have

$$U = U_0 + (U_1 - U_0)\frac{w}{w_1} \quad (8)$$

with

$$U_0 = \tfrac{1}{2}(nR\gamma_0),\ U_1 = \tfrac{1}{2}(nR\gamma_1) \quad (9)$$

The linearity of Eq. (7) and (8) with respect to $w$ is of course a hypothesis. To determine $\gamma$ at intermediate water contents would be more difficult than the present tests. Providing control of the environmental relative humidity at arbitrary temperature would not be difficult; however, creating and maintaining a uniform value of some intermediate water content in the specimen would. It takes a very long time to dry a specimen to a uniform moisture content, and due to the coupling of temperature and humidity changes, it appears rather difficult to maintain a constant and uniform moisture content during the test. It would probably be necessary to make inferences from tests on specimens that are in a transient hygrothermal state. The advantage of the tests at either perfect saturation or perfect dryness is that a uniform moisture state is easily obtained and easily maintained at temperature changes.

That the activation energy should depend on the moisture content is not surprising. It is well established

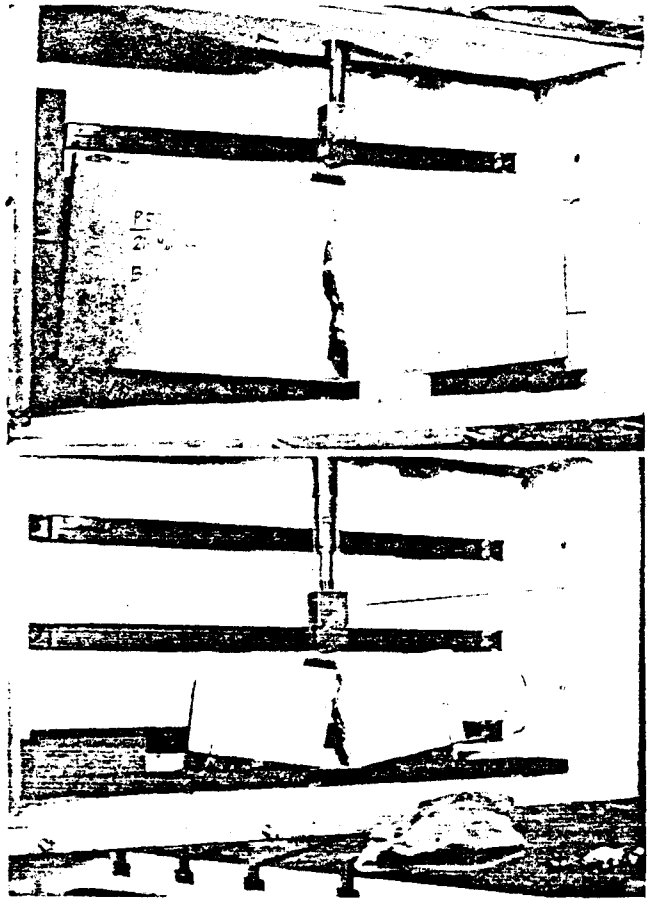

*Fig. 7—Loaded specimens in an oven, installed in the testing machine*

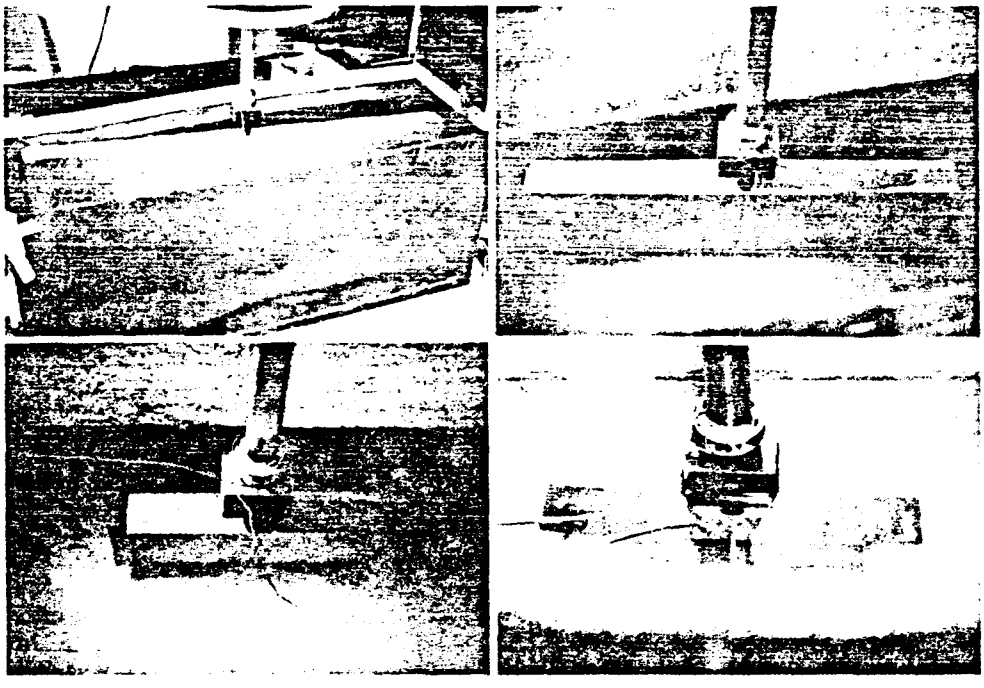

*Fig. 8—Loaded specimens in the water tank*

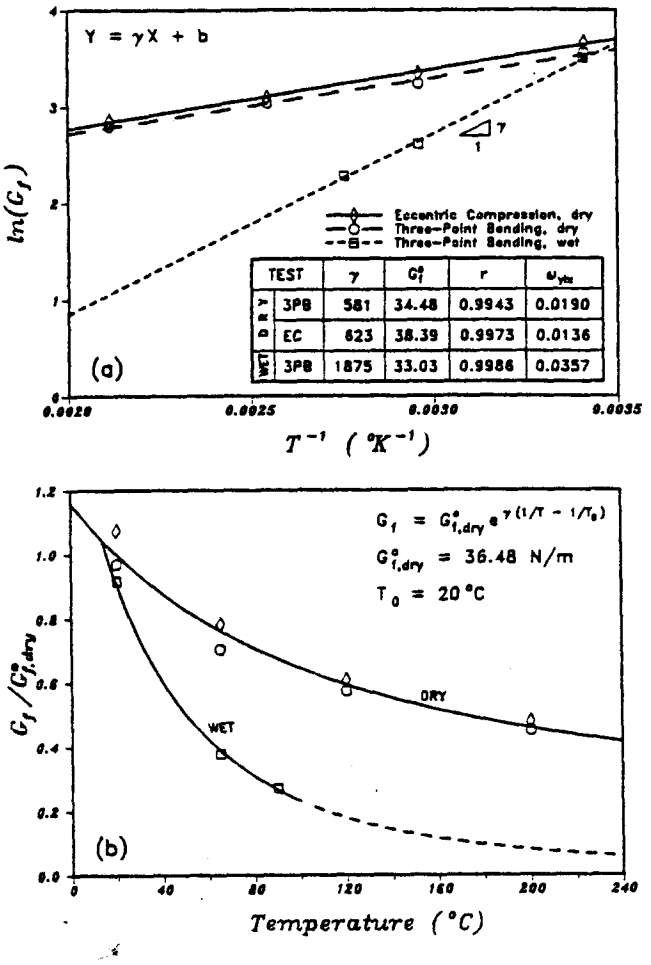


*Fig. 9—Experimental results and theoretical formula for the effect of temperature on fracture energy for both dry and wet specimens: (a) linear regression lines; and (b) fracture energy versus temperature ($\gamma$ = activation temperature in degrees K, $G_f^\circ$ = fracture energy at reference temperature $T_0$ = 20 C in N/m)*

that the activation energy of concrete creep strongly varies with the moisture content, and the same is true of other porous hydrophylic materials such as wood. Also, the creep activation energy is known to depend on $w$ nearly linearly.

The physical explanation of the dependence of $U$ on $w$ lies probably in the very high disjoining pressures caused by layers of hindered adsorbed water or interlayer water within the finest pores of the cement gel. These pressures are superimposed on the stresses due to load, thus lowering the energy barrier for bond ruptures. A mathematical model based on this mechanism would no doubt be of help for determining the dependence of $U$ on $w$ more accurately and for interpreting test results at intermediate values of $w$.

## CONCLUSIONS

1. The size effect law is applicable not only at room temperature but also at elevated temperatures up to 200 C (392 F). Its parameters depend on temperature as well as specific water content of concrete.

2. The Mode I fracture energy of concrete significantly depends on temperature $T$. It decreases monotonically and smoothly as $T$ increases. For concrete near saturation water content, this dependence is more pronounced than for predried concrete.

3. The effect of specific water content on the fracture energy is small at room temperature but grows as temperature increases and is very large at temperatures close to 100 C (212 F).

4. The measured dependence of Mode I fracture energy on temperature agrees with Bažant's[8] formula [Eq. (5)] based on the activation energy theory (rate-process theory).

5. Very different types of specimens such as the three-point bend and eccentric compression specimens yield approximately the same fracture energy values at various temperatures. This indicates that the present results for the fracture energy should represent true material properties.

**Table 3 — Fracture energy values obtained from tests, N/m***

| Test | Age | 20 C (68 F) | 65 C (149 F) | 90 C (194 F) | 120 C (248 F) | 200 C (392 F) |
|---|---|---|---|---|---|---|
| 3-point bend, dry | 28 | 35.24 | 25.58 | — | 20.87 | 16.39 |
| Eccentric compression, dry | 28 | 39.01 | 28.42 | — | 22.06 | 17.36 |
| 3-point bend, wet | 28† | 33.30‡ | 13.72† | 9.79† | — | — |
| 3-point bend, wet | 41 | — | 14.57 | 10.40 | — | — |

* 1 N/m = 0.005710 lb./in.
† Corrected from age 41 days.
‡ From Bažant and Pfeiffer, not in water bath but in air immediately after removal from moist room.


## ACKNOWLEDGMENTS

Grateful acknowledgment is due to the U.S. Air Force Office of Scientific Research (Contract No. F49620-87-C-0030DEF with Northwestern University, monitored by Dr. Spencer T. Wu) for partial support of the theoretical work and measurements, and for the preparation of specimens for the cooperative project between Universidad Politécnica de Madrid, Spain, and Northwestern University, funded under the U.S.-Spanish treaty (Grant CCA-8309071).


## REFERENCES


1. Tetelman, A. S., and McEvily, A. J., *Fracture of Structural Materials*, John Wiley & Sons, New York, 1967, pp. 274-276.

2. Kanninen, M. F., and Popelar, C. H., *Advanced Fracture Mechanics*, Oxford University Press, New York, 1985, pp. 17-18, 26-30, and 82.

3. Cherepanov, G. P., *Mechanics of Brittle Fracture*, McGraw-Hill Book Co., New York, 1979 (translated from the Russian original published by Nauka, Moscow, 1974), pp. 174 and 455.

4. Hillerborg, A.; Modéer, M.; and Petersson, P.E., "Analysis of Crack Formation and Crack Growth in Concrete by Means of Fracture Mechanics and Finite Elements," *Cement and Concrete Research*, V. 6, No. 6, Nov. 1976, pp. 773-781.

5. Hillerborg, A., "The Theoretical Basis of a Method to Determine the Fracture Energy $G_f$ of Concrete," *Materials and Structures, Research and Testing* (RILEM, Paris), V. 18, No. 106, July-Aug. 1985, pp. 291-296.

6. Bažant, Z. P., "Fracture Mechanics and Strain-Softening of Concrete," *Preprints*, U.S.-Japan Seminar on Finite Element Analysis of Reinforced Concrete Structures, Japan Society for the Promotion of Science, Tokyo, May 1985, pp. 71-92.

7. Bažant, Z. P., "Fracture in Concrete and Reinforced Concrete," *Mechanics of Geomaterials: Rocks, Concrete, Soils*, John Wiley & Sons, Chichester, 1985, pp. 259-304.

8. Bažant, Z. P., "Fracture Energy of Heterogeneous Materials

and Similitude," *Preprints*, International Conference on Fracture of Concrete and Rock (Houston, June 1987), Society for Experimental Mechanics, Bethel, 1987, pp. 390-402.

9. Bažant, Zdeněk P.; Kim, Jin-Keun; and Pfeiffer, Phillip A., "Nonlinear Fracture Properties from Size Effect Tests," *Journal of Structural Engineering*, ASCE, V. 112, No. 2, Feb. 1986, pp. 289-307.

10. Bažant, Z. P.; Kim, J.-K.; and Pfeiffer, P. A., "Determination of Nonlinear Fracture Parameters from Size Effect Tests," NATO Advanced Research Workshop on Application of Fracture Mechanics to Cementitious Composites, Northwestern University, Evanston, Sept. 1984, pp. 143-169.

11. Bažant, Zdeněk P., "Size Effect in Blunt Fracture: Concrete, Rock, and Metal," *Journal of Engineering Mechanics*, ASCE, V. 110, No. 4, Apr. 1984, pp. 518-535.

12. Bažant, Z. P.; Sener, S.; and Prat, P. C., "Size Effect Tests of Torsional Failure of Concrete Beams," *Report* No. 86-12/428s, Center for Concrete and Geomaterials, Northwestern University, Evanston, Dec. 1986, 18 pp.

13. Bažant, Zdeněk P.; and Kim, Jin-Keun, "Size Effect in Shear Failure of Longitudinally Reinforced Beams," ACI JOURNAL, *Proceedings* V. 81, No. 5, Sept.-Oct. 1984, pp. 456-468.

14. Bažant, Zdeněk P., and Cao, Zhiping, "Size Effect in Punching Shear Failure of Slabs," *ACI Structural Journal*, V. 84, No. 1, Jan.-Feb. 1987, pp. 44-53.

15. Bažant, Z. P., and Pfeiffer, P. A., "Shear Fracture Tests of Concrete," *Materials and Structures, Research and Testing* (RILEM, Paris), V. 19, No. 110, Mar.-Apr. 1986, pp. 111-121.

16. Bažant, Zdeněk P., and Thonguthai, Werapol, "Pore Pressure and Drying of Concrete at High Temperature," *Proceedings*, ASCE, V. 104, EM5, Oct. 1978, pp. 1059-1079.

17. Bažant, Zdeněk P., and Panula, Liisa, "Statistical Stability Effects in Concrete Failure," *Proceedinngs*, ASCE, V. 104, EM5, Oct. 1978, pp. 1195-1212.

18. Neville, A. M., *Properties of Concrete*, 3rd Edition, Pitman Publishing Limited, London, 1981, 779 pp.

19. Broek, D., *Elementary Engineering Fracture Mechanics*, Sijthoff and Noordhoff, International Publishers, Netherlands, 1978, 408 pp.

20. Knott, J. F., *Fundamentals of Fracture Mechanics*, Butterworths, London, 1973, 273 pp.

21. Tada, H.; Paris, P. C.; and Irwin, G. R., *The Stress Analysis of Cracks Handbook*, Del Research Corp., Hellertown, 1973.

22. Bažant, Zdeněk P., and Oh, B. H., "Crack Band Theory for Fracture of Concrete," *Materials and Structures, Research and Testing* (RILEM, Paris), V. 16, No. 93, May-June 1983, pp. 155-177.

23. Cottrell, A. H., *The Mechanical Properties of Matter*, John Wiley & Sons, New York, 1964, 430 pp.

24. Evans, A. G., and Fu, Y., "The Mechanical Behavior of Alumina," *Fracture in Engineering Materials*, Noyes Publications, Park Ridge, p. 71.

25. Thouless, M. D.; Hsueh, C. H.; and Evans, A. G., "A Damage Model of Creep Crack Growth in Polycrystals," *Acta Metallurgica*, V. 31, No. 10, 1983, pp. 1675-1687.